

# Multiple Enone-Directed Reactivity Modes Lead to the Selective Photochemical Fluorination of Polycyclic Terpenoid Derivatives

Cody Ross Pitts,<sup>1b</sup> Desta Doro Bume, Stefan Andrew Harry, Maxime A. Siegler, and Thomas Lectka\*

Department of Chemistry, Johns Hopkins University, 3400 N. Charles Street, Baltimore, Maryland 21218, United States

**S** Supporting Information

**ABSTRACT:** In the realm of aliphatic fluorination, the problem of reactivity has been very successfully addressed in recent years. In contrast, the associated problem of selectivity, that is, directing fluorination to specific sites in complex molecules, remains a great, fundamental challenge. In this report, we show that the enone functional group, upon photoexcitation, provides a solution. Based solely on orientation of the oxygen atom, site-selective photochemical fluorination is achieved on steroids and bioactive polycycles with up to 65 different  $sp^3$  C—H bonds. We have also found that  $\gamma$ -,  $\beta$ -, homoallylic, and allylic fluorination are all possible and predictable through the theoretical modes reported herein. Lastly, we present a preliminary mechanistic hypothesis characterized by intramolecular hydrogen atom transfer, radical fluorination, and ultimate restoration of the enone. In all, these results provide a leap forward in the design of selective fluorination of complex substrates that should be relevant to drug discovery, where fluorine plays a prominent role.

Reactivity and selectivity define two central challenges in aliphatic C—H bond functionalization. In the domain of aliphatic fluorination, recent advances in reactivity beyond the reliance on harsh reagents such as fluorine gas are notable.<sup>1</sup> Since the advent of metal-catalyzed  $sp^3$  C—H fluorination in 2012,<sup>2</sup> we, and others, have developed several user-friendly examples of aliphatic fluorination reactions using transition metal catalysts,<sup>3</sup> organocatalysts,<sup>4</sup> radical initiators,<sup>5</sup> and photosensitizers,<sup>6</sup> putting controllable “radical fluorination” within arm’s reach. However, using these methods, selectivity is still quite limited to smaller molecules of high symmetry and to those with more acidic C—H bonds adjacent to aromatic rings or activated by chelating auxiliaries.<sup>7,8</sup> In a few cases, selective fluorination has been observed on more intricate substrates, but it is usually in a serendipitous and unpredictable fashion. More often, the subsection of molecules with large numbers of dissimilar C—H bonds to these procedures results in a large number of fluorinated products. Given the growing importance of fluorinated molecules in medicine,<sup>9</sup> among areas of biology, agrochemistry, and materials science, the leap toward predictable, site-selective  $sp^3$  C—H fluorination on complex molecules is both timely and necessary.

Accordingly, we show that the enone functional group, upon photoexcitation, can direct  $sp^3$  C—H fluorination with a high degree of predictability in less than 4 h. By the placement of the

enone oxygen at various positions in steroids and other bioactive polycycles, different sites can be fluorinated selectively that otherwise would be inaccessible on substrates with as many as 65  $sp^3$  C—H bonds. Notably, steroidal and other terpenoidal enones constitute a number of drugs on the market and in clinical trials (in part, due to improved physicochemical and pharmacokinetic properties over nonoxidized counterparts<sup>10</sup>), asserting them as desirable targets for fluorine installation. In addition, we have found that the enone group can direct either  $\gamma$ - or  $\beta$ -fluorination through a number of modes that involve different transition state conformations, ring sizes, and C=C bond positioning. Here, the strict proclivity for  $\gamma$ - or  $\beta$ -hydrogen atom abstraction is surprising, given the ability of enone photoexcitation to promote  $\alpha$ -cleavage (Norrish I),  $\beta$ -cleavage (Norrish II), cyclization (Norrish–Yang), geometric isomerization, dimerization, and electron transfer chemistry, among other reactions.<sup>11</sup> Furthermore, we demonstrate the ability to predict <sup>19</sup>F NMR shifts using DFT calculations to assist in product characterization prior to isolation. Finally, we offer preliminary insight on the putative enone-assisted hydrogen atom transfer mechanism.

As this method can be used to access a variety of C—H sites through well-defined reactivity modes, we offer a classification system for the anticipated products of an enone-directed photochemical fluorination based on proximity of the C=C bond to the reaction site and the conformation of the transition state (Figure 1). Mode I and mode II represent reactions that proceed through 6-membered transition states with the placement of the enone C=C bond distal and proximal, respectively, to the fluorination site. Interestingly, mode III and mode IV represent reactions that proceed through 5-membered transition states and are also compatible with distal and proximal C=C bond placement. Note that the proximal mode II and mode IV are distinguished from distal modes because the products represent chemically distinct homoallylic and allylic fluorides. In all, we have found these four reactivity modes to be predictable and directly applicable to targeting previously inaccessible fluorination sites on biologically relevant terpenoids and derivatives thereof.<sup>12</sup> What is more, the reaction is operationally simple and mindful of principles of green chemistry, requiring only the enone, Selectfluor, and mid- to near-ultraviolet light (see conditions in Table 1).

The most abundant or easily accessible enones on polycycles are those primed for C—H fluorination through the 6-membered transition state (modes I and II); thus, the

Received: January 11, 2017

Published: February 1, 2017



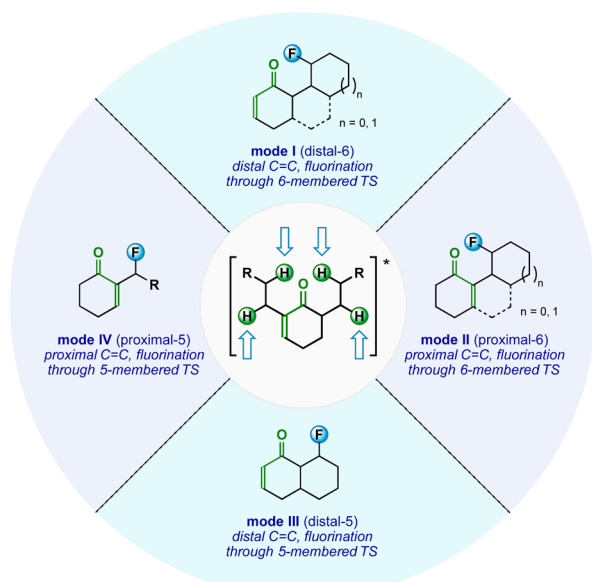
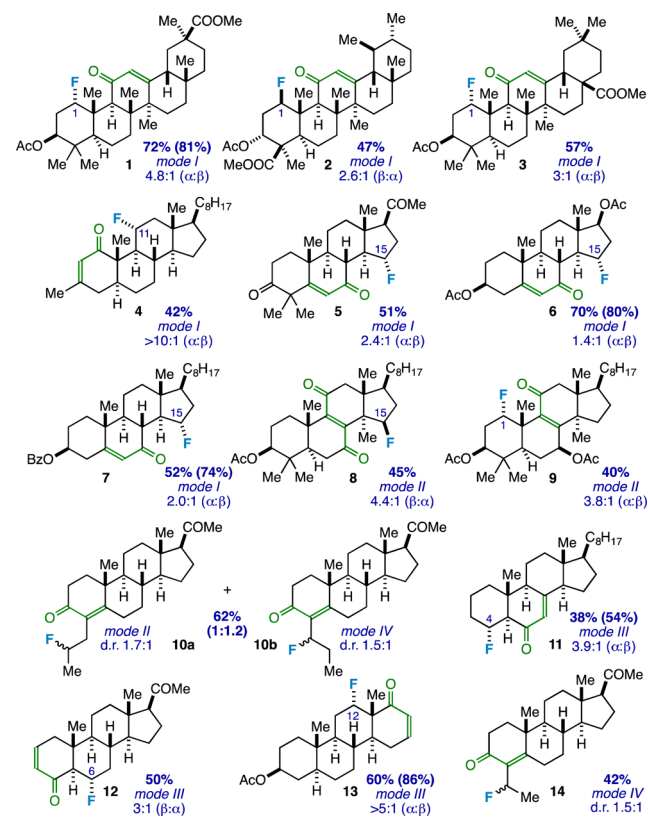


**Figure 1.** Classification of reactivity modes (I–IV) that lead to selective  $\gamma$ -,  $\beta$ -, homoallylic, and allylic photochemical fluorination.

corresponding  $\gamma$ -fluorination products comprise the majority of Table 1. The starting materials for compounds 1–3 represent derivatives of the pentacyclic triterpenoids 18- $\beta$ -glycyrrhetic acid, boswellic acid, and oleanolic acid, with the enone located on the C-ring poised for mode I fluorination on the A-ring (analogs of these molecules have been shown to exhibit numerous pharmacological properties, including anti-inflammatory,<sup>13</sup> anticancer,<sup>14</sup> anti-HIV,<sup>15</sup> and anti-HCV<sup>16</sup>). The predicted fluorinated products at the C1 position were obtained in good yields (up to 72%) with a preference for the  $\alpha$ -isomer in 1 and 3 and the  $\beta$ -isomer in 2. Upon isolation, the site of fluorination for each product was confirmed by (1) relocation of the distinct equatorial C1 hydrogen atom in the <sup>1</sup>H NMR spectrum (dt at  $\sim$ 2.8 ppm) of the starting material to the appropriate chemical shift and splitting of a hydrogen atom geminal to fluorine, (2) <sup>2</sup>J<sub>CF</sub> and <sup>3</sup>J<sub>CF</sub>-coupling to distinguishable peaks in the <sup>13</sup>C NMR spectrum (see SI for details), and (3) comparison to the calculated <sup>19</sup>F NMR shifts using an empirical equation developed in our laboratory.<sup>17</sup> If the enone is placed instead on the A-ring, poised for mode I fluorination on the C-ring (compound 4), selective fluorination at the C11 position can be achieved. In this instance, we determined the  $\alpha$ -isomer to be the major diastereomer and have identified the fluorination site as stated above.

We also investigated mode I fluorination of the D-ring at the C15 position by placing the enone group on the B-ring of derivatives of bioactive steroids such as progesterone, testosterone acetate, and cholesterol (compounds 5–7). In fact, fluorination on the five-membered ring occurs in up to 70% yield ( $\alpha$ -isomer favored), as confirmed by chemical shift and <sup>2</sup>J<sub>HF</sub>-coupling in the <sup>19</sup>F NMR spectra (>50 Hz is typical for cyclopentane ring fluorination) followed by <sup>13</sup>C NMR analysis of the products. Furthermore, crystals were grown of compound 5 through solvent evaporation that proved suitable for X-ray structure determination (Table S1). To the best of our knowledge, the C15 position is an unprecedented site of fluorination, and thus, products of this reaction could be interesting candidates for studying structure–activity relationships and pharmacological properties.<sup>18</sup>

**Table 1.** Directed Photochemical sp<sup>3</sup> C–H Fluorination of Bioactive Polycyclic Terpenoid Derivatives



In lanosterol derivatives 8 and 9, enones were shown to direct homoallylic (mode II) fluorination at the C15 and C1 positions, respectively, through similar transition states. Interestingly, enedione 8 can undergo fluorination at either position, yet favors functionalization of the C15 position (here, the  $\beta$ -isomer is preferred, likely due to the vicinal methyl group on the bottom face). We attribute the observed selectivity to the “polar effect”; that is, the inductive effect from the electron-withdrawing group at the C3 position (acetate) decreases the reactivity of the C1 hydrogen atoms relative to those at the C15 position toward abstraction. This phenomenon is well preceded in radical-based hydrogen atom abstractions.<sup>19</sup> Notably, if the option to fluorinate the C15 position is removed, fluorination will still occur three bonds away at C1 (9). However, if an electron-withdrawing group (for instance, an acetate or a carbonyl) is present two bonds from the fluorination site, we have found that reactivity is suppressed.

In addition to 5- and 6-membered ring fluorination on polycyclic cores, we discovered that the reaction is amenable to mode II side-chain fluorination. Running the reaction on a progesterone derivative with an *n*-propyl group in the C4 position, we discovered the anticipated homoallylic fluoride along with the unexpected allylic fluoride in near equal ratios ( $\sim$ 1:1.2 10a:10b) by <sup>19</sup>F NMR analysis. This result prompted an investigation of fluorination through less common 5-membered transition states to, at the very least, double the number of accessible fluorination sites on steroids (and other polycycles) using this method.

The starting enones for 11, 12, and 13 were synthesized in order to determine the viability of fluorination through 5-membered transition states with the C=C bond distal to the reaction site (mode III). In fact, mode III fluorination in up to

60% yield was achieved on the decalin-like substructures that permit selective  $\beta$ -functionalization on the C4 (**11**, A-ring,  $\alpha$ -isomer favored), C6 (**12**, B-ring,  $\alpha$ -isomer favored), and C12 (**13**, C-ring,  $\alpha$ -isomer favored) positions by  $^{19}\text{F}$ ,  $^1\text{H}$ , and  $^{13}\text{C}$  NMR analyses. Finally, the aforementioned result of the *n*-propylated progesterone suggested one more reactivity mode, mode IV, which would allow access to allylic fluorides. An ethylated analog was synthesized that underwent mode IV fluorination exclusively in the allylic position (**14**), with no primary fluoride observed from a mode II reaction. Allylic fluorination on the secondary position was also favored over homoallylic fluorination on the tertiary position of an isobutyl-substituted progesterone (not shown in Table 1), albeit the reaction proceeded in poor yield. Nevertheless, this result is significant in establishing basic reactivity trends such that secondary > tertiary and primary carbon fluorination sites.

As a testament to the selectivity of the reaction, we subjected triterpenoid saponin derivative **15** to photochemical fluorination. Even in the presence of 65 distinct  $\text{sp}^3$  C—H bonds, the enone functional group very effectively directs fluorination to the C1 position in 41% yield (Figure 2). Here, and in most

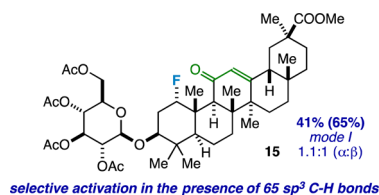


**Figure 2.** Fluorination of triterpenoid saponin derivative **15** in an extreme illustration of selectivity.

cases (modes I–IV), it is important to note that the majority of the mass balance can be accounted for with recovered starting material and very minor fluorinated byproducts through NMR analyses of the crude reaction mixture. Though, in some cases, we have identified slight, competitive fluorination directed by ketones (for example, compounds **5**, **10**, **12**, and **14**). From another vantage point, we have found preliminary success in the fluorination of simpler enone substrates, e.g., 2-butylcyclohexa-2-en-1-one (predominately mode IV) and piperitone (mode III), albeit in lower yields. In general, we note that the method is better primed for rigid structures, regardless of complexity.

Finally, we present a preliminary mechanistic hypothesis (Figure 3). Regarding reaction initiation, we addressed the role of photochemistry with a number of control experiments. To rule out thermal processes, reactions were performed at the operating temperature of the Rayonet reactor ( $\sim 40^\circ\text{C}$ ), but they provided no fluorinated products (although, at reflux, note that a large distribution of different fluorinated products is

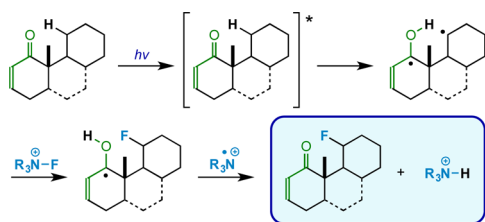


**Figure 3.** Preliminary mechanistic hypothesis for enone-directed photochemical  $\text{sp}^3$  C—H fluorination using Selectfluor.

observed<sup>20</sup>). The UV–vis spectra of Selectfluor and the enone-containing substrates reveal that Selectfluor has no absorbance above the Pyrex cutoff (ca. 275 nm)<sup>21</sup> and the substrates typically absorb between 275 and 380 nm; therefore, the substrates contain the only possible chromophores under our reaction conditions. Literature precedent suggests that excited enones experience rapid intersystem crossing from the singlet state ( $S_1$ ) to the triplet state ( $T_1$ ), and that enones with  $n \rightarrow \pi^*$  lowest-energy  $T_1$  states can undergo hydrogen atom abstraction.<sup>11</sup> If a triplet mechanism is at play, we should be able to effect the reaction with a triplet sensitizer. Accordingly, if the reaction is run using cool white LEDs (cutoff at ca. 400 nm), no fluorinated products are observed. Yet if the same reaction is performed in the presence of 9-fluorenone, a known triplet sensitizer with absorbance above 400 nm,<sup>22</sup> the desired fluorinated products are observed. Thus, we can conclude that enone photochemistry plays a crucial role in the mechanism and reactivity likely occurs from  $T_1$ .

An intramolecular hydrogen atom abstraction directed by the  $T_1$  excited enone would explain the observed selectivity.<sup>23</sup> In fact, we have calculated transition states for intramolecular 1,4- and 1,5-hydrogen atom transfer at B3LYP/6-311++G\*\* (activation energies ( $E_a$ ) of 9.1 and 9.8 kcal/mol, respectively) that suggest these are reasonable processes. Beyond this step, the translocated, carbon-centered radical is susceptible to fluorination in the presence of Selectfluor, which is known to react with free radicals very rapidly.<sup>24</sup> The Selectfluor-derived byproduct of this step, the *N*-centered radical, could conceivably undergo hydrogen atom transfer from the oxygen atom to regenerate the carbonyl carbon and terminate the *N*-centered radical. To probe the role of the *N*-centered radical, we generated it in the dark using the established triethylborane method<sup>5</sup> and examined the  $^{19}\text{F}$  NMR spectrum of the reaction mixture. Note that we have previously shown that this intermediate is responsible for C—H cleavage,<sup>25</sup> as well as oxidation,<sup>21</sup> in radical chain fluorination reactions, but its role as a chain propagator seems unlikely here. As anticipated, a triethylborane-initiated reaction resulted in minor  $\text{sp}^3$  C—H fluorination, but did not provide similar fluorinated products, yields, or selectivity. Thus, if the *N*-centered radical is formed under photochemical conditions, it is necessarily playing a different role, that is, likely, hydrogen atom transfer from the oxygen to restore the enone in the final step. In all, this appears to be a reasonable mechanism; however, enone photochemistry is generally complicated. Thus, at this time it is difficult to rule out the possibility of electron transfer chemistry playing a role.

Considering the complexity of enone photochemistry, the ability to direct  $\text{sp}^3$  C—H fluorination on such intricate molecules is a surprising and notable result. The reaction is relatively fast, simple, and predictable, thus paving clear paths to new late-stage fluorination products. In addition, this method has effectively quadrupled the number of accessible C—H sites for aliphatic fluorination on steroids. Accordingly, we anticipate near-term adoption of this method in a medicinal chemistry setting, and we hope it will encourage the exploration of additional enone-directed functionalization and corresponding mechanistic elucidation.

## ■ ASSOCIATED CONTENT

### Supporting Information

The Supporting Information is available free of charge on the ACS Publications website at DOI: 10.1021/jacs.7b00335.



Experimental procedures, spectra, computational data, and crystallographic data (PDF)  
Data for C<sub>23</sub>H<sub>31</sub>FO<sub>3</sub> (CIF)

## AUTHOR INFORMATION

### Corresponding Author

\*lectka@jhu.edu

### ORCID

Cody Ross Pitts: 0000-0003-1047-8924

### Notes

The authors declare no competing financial interest.

## ACKNOWLEDGMENTS

T.L. thanks the National Science Foundation (NSF) (CHE-1465131) for support. C.R.P. thanks Johns Hopkins for a Glen E. Meyer '39 Fellowship. The authors also thank Rayyan Trebonias Jokhai, Benjamin H. Park, Hunter W. Pool, and Javier A. Casado-Cocero for their assistance, as well as COSMIC Lab (Old Dominion University) and Ananya Majumdar (Johns Hopkins University).

## REFERENCES

- (1) Champagne, P. A.; Desroches, J.; Hamel, J.-D.; Vandamme, M.; Paquin, J.-F. *Chem. Rev.* **2015**, *115*, 9073–9174.
- (2) (a) Liu, W.; Huang, X.; Cheng, M.-J.; Nielsen, R. J.; Goddard, W. A., III; Groves, J. T. *Science* **2012**, *337*, 1322–1325. (b) Bloom, S.; Pitts, C. R.; Miller, D. C.; Haselton, N.; Holl, M. G.; Urheim, E.; Lectka, T. *Angew. Chem., Int. Ed.* **2012**, *51*, 10580–10583.
- (3) (a) Bloom, S.; Pitts, C. R.; Woltornist, R.; Griswold, A.; Holl, M. G.; Lectka, T. *Org. Lett.* **2013**, *15*, 1722–1724. (b) Liu, W.; Groves, J. T. *Angew. Chem., Int. Ed.* **2013**, *52*, 6024–6027. (c) Xia, J.-B.; Ma, Y.; Chen, C. *Org. Chem. Front.* **2014**, *1*, 468–472.
- (4) Amaoka, Y.; Nagatomo, M.; Inoue, M. *Org. Lett.* **2013**, *15*, 2160–2163.
- (5) Pitts, C. R.; Ling, B.; Woltornist, R.; Liu, R.; Lectka, T. *J. Org. Chem.* **2014**, *79*, 8895–8899.
- (6) (a) Xia, J.-B.; Zhu, C.; Chen, C. *J. Am. Chem. Soc.* **2013**, *135*, 17494–17500. (b) Bloom, S.; Knippel, J. L.; Lectka, T. *Chem. Sci.* **2014**, *5*, 1175–1178. (c) Kee, C. W.; Chin, K. F.; Wong, M. W.; Tan, C.-H. *Chem. Commun.* **2014**, *50*, 8211–8214. (d) Xia, J.-B.; Zhu, C.; Chen, C. *Chem. Commun.* **2014**, *50*, 11701–11704. (e) Halperin, S. D.; Fan, H.; Chang, S.; Martin, R. E.; Britton, R. *Angew. Chem., Int. Ed.* **2014**, *53*, 4690–4693. (f) Rueda-Becerril, M.; Mahe, O.; Drouin, M.; Majewski, M. B.; West, J. G.; Wolf, M. O.; Sammis, G. M.; Paquin, J.-F. *J. Am. Chem. Soc.* **2014**, *136*, 2637–2641. (g) West, J. G.; Bedell, T. A.; Sorensen, E. J. *Angew. Chem., Int. Ed.* **2016**, *55*, 8923–8927. (h) Bume, D. D.; Pitts, C. R.; Jokhai, R. T.; Lectka, T. *Tetrahedron* **2016**, *72*, 6031–6036.
- (7) (a) Zhu, R.-Y.; Tanaka, K.; Li, G.-C.; He, J.; Fu, H.-Y.; Li, S.-H.; Yu, J.-Q. *J. Am. Chem. Soc.* **2015**, *137*, 7067–7070. (b) Zhang, Q.; Yin, X.-S.; Chen, K.; Zhang, S.-Q.; Shi, B.-F. *J. Am. Chem. Soc.* **2015**, *137*, 8219–8226. (c) Miao, J.; Yang, K.; Kurek, M.; Ge, H. *Org. Lett.* **2015**, *17*, 3738–3741. (d) Lu, X.; Xiao, B.; Shang, R.; Liu, L. *Chin. Chem. Lett.* **2016**, *27*, 305–311.
- (8) Amidyl radical-based remote C–H fluorination reactions have also been reported, but with limited scope: (a) Li, Z.; Song, L.; Li, C. *J. Am. Chem. Soc.* **2013**, *135*, 4640–4643. (b) Groendyke, B. J.; AbuSalim, D. I.; Cook, S. P. *J. Am. Chem. Soc.* **2016**, *138*, 12771–12774.
- (9) Purser, S.; Moore, P. R.; Swallow, S.; Gouverneur, V. *Chem. Soc. Rev.* **2008**, *37*, 320–330.
- (10) Michaudel, Q.; Journot, G.; Regueiro-Ren, A.; Goswami, A.; Guo, Z.; Tully, T. P.; Zou, L.; Ramabhadran, R. O.; Houk, K. N.; Baran, P. S. *Angew. Chem., Int. Ed.* **2014**, *53*, 12091–12096.
- (11) Turro, N. J.; Scaiano, J. C.; Ramamurthy, V. *Modern Molecular Photochemistry of Organic Molecules*; University Science Books: Sausalito, CA, 2010.
- (12) Predictability and selectivity are aided by structural rigidity of the substrates.
- (13) Han, N.; Bakovic, M. *J. Bioanal. Biomed.* **2015**, *S12*, 1–11.
- (14) Petronelli, A.; Pannitteri, G.; Testa, U. *Anti-Cancer Drugs* **2009**, *20*, 880–892.
- (15) Cassels, B. K.; Asencio, M. *Phytochem. Rev.* **2011**, *10*, 545–564.
- (16) Yu, F.; Wang, Q.; Zhang, Z.; Peng, Y.; Qiu, Y.; Shi, Y.; Zheng, Y.; Xiao, S.; Wang, H.; Huang, X.; Zhu, L.; Chen, K.; Zhao, C.; Zhang, C.; Yu, M.; Sun, D.; Zhang, L.; Zhou, D. *J. Med. Chem.* **2013**, *56*, 4300–4319.
- (17) At B3LYP/6-311++G\*\*, we performed geometry optimizations on a number of fluorinated products in Gaussian, followed by NMR calculations using the CSGT method. After compiling the calculated isotropic shifts for the fluorine atoms, we performed a simple linear regression analysis between these isotropic shifts ( $\delta_{\text{iso}}$ ) and experimentally observed chemical shifts in the <sup>19</sup>F NMR spectra ( $\delta_{\text{obs}}$ ). In doing so, we established an empirical equation that was used to predict the <sup>19</sup>F NMR shift ( $\delta_{\text{calc}}$ ) of a desired polycyclic product within an average of  $0.6 \pm 0.5$  ppm ( $|\delta_{\text{obs}} - \delta_{\text{calc}}|$ ), which is significant in light of the large <sup>19</sup>F NMR chemical shift range (Table S2). The equation was also helpful in assigning stereochemistry of the diastereomers prior to isolation and full characterization.
- (18) Kumagai, G.; Takano, M.; Shindo, K.; Sawada, D.; Saito, N.; Saito, H.; Kakuda, S.; Takagi, K.-I.; Takimoto-Kamimura, M.; Takenouchi, K.; Chen, T. C.; Kittaka, A. *Anticancer Res.* **2012**, *32*, 311–317.
- (19) (a) Walling, C. *Free Radicals in Solution*; Wiley: New York, NY, 1957. (b) Zavitsas, A. A.; Pinto, J. A. *J. Am. Chem. Soc.* **1972**, *94*, 7390–7396. (c) Newhouse, T.; Baran, P. S. *Angew. Chem., Int. Ed.* **2011**, *50*, 3362–3374.
- (20) Chambers, R. D.; Parsons, M.; Sandford, G.; Bowden, R. *Chem. Commun.* **2000**, 959–960.
- (21) Pitts, C. R.; Ling, B.; Snyder, J. A.; Bragg, A. E.; Lectka, T. *J. Am. Chem. Soc.* **2016**, *138*, 6598–6609.
- (22) Valentine, D., Jr.; Hammond, G. S. *J. Am. Chem. Soc.* **1972**, *94*, 3449–3454.
- (23) For examples of selective C–H functionalization achieved through stepwise Norrish–Yang cyclization and oxidation/iodination, see: (a) Wehrli, H.; Heller, M. S.; Schaffner, K.; Jeger, O. *Helv. Chim. Acta* **1961**, *44*, 2162–2173. (b) Renata, H.; Zhou, Q.; Baran, P. S. *Science* **2013**, *339*, 59–63.
- (24) Rueda-Becerril, M.; Sazepin, C. C.; Leung, J. C. T.; Okbinoglu, T.; Kennepohl, P.; Paquin, J.-F.; Sammis, G. M. *J. Am. Chem. Soc.* **2012**, *134*, 4026–4029.
- (25) Pitts, C. R.; Bloom, S.; Woltornist, R.; Auvenshine, D. J.; Ryzhkov, L. R.; Siegler, M. A.; Lectka, T. *J. Am. Chem. Soc.* **2014**, *136*, 9780–9791.